Ivo DOLEŽEL[1], Bohuš ULRYCH[2], Petr KROPÍK[2]

Academy of Sciences of the Czech Republic, Praha, Czech Republic (1), University of West Bohemia in Plzeň, Czech Republic (2)

T-potential based model of induction heating of thin conductive plates in hard-coupled formulation

Abstract. *Mathematical and computer models of induction heating of very thin plates are presented. The plate is supposed to be exposed by time-variable external magnetic field. Distribution of eddy currents and other quantities is modeled in terms of electric vector potential. The problem is solved in hard-coupled formulation and the methodology is illustrated by a typical example.*

Streszczenie. *Zaprezentowano model matematyczny i model komputerowy dla problem grzania indukcyjnego bardzo cienkich płytek. Płytka wystawiona jest na działanie zmiennego pola magnetycznego. Rozkład gęstości prądów wirowych i inne wielkości zostały zamodelowane poprzez użycie elektrycznego potencjału wektorowego T. Problem został rozwiązany w warunkach silnego sprzężenia elektromagnetyczno-cieplnego a przedstawiona metodyka zilustrowana jest prostym przykładem. (**Model grzania indukcyjnego cienkich płytek bazujący na potencjale T przy silnym sprzężeniu zjawisk**)*

Keywords: induction heating, *T*-potential, hard-coupled formulation, numerical analysis.
Słowa kluczowe: grzanie indukcyjne, potencjał T, silne sprzężenie, analiza numeryczna

Introduction

Nowadays, modeling of induction heating is usually performed numerically using the finite element method [1–3] and magnetic field in the system is described in terms of the magnetic vector potential $\boldsymbol{A}$. This approach is also implemented into a number of professional codes such as OPERA [4], ANSYS [5] or FLUX [6].

From time to time, however, one must solve problems where this classical approach can fail. One class of such problems is characterized by geometrical incommensurability of some parts of the investigated system. This means that one dimension of such a part is much smaller than other dimensions, but yet, this dimension is important and its influence cannot be neglected. We can mention, for example, local induction heating of nonferromagnetic thin plates. One of the possible arrangements for realizing this technological process is depicted in Fig. 1. A nonferromagnetic plate **1** of an arbitrary shape and very small thickness δ is locally heated by eddy currents generated by time-varying magnetic field $\boldsymbol{B}_{\mathrm{ext}}(t)$ produced in magnetic circuit **2** by field coil **3** and concentrated by appropriately shaped magnetic focusators **4.1** and **4.2**.

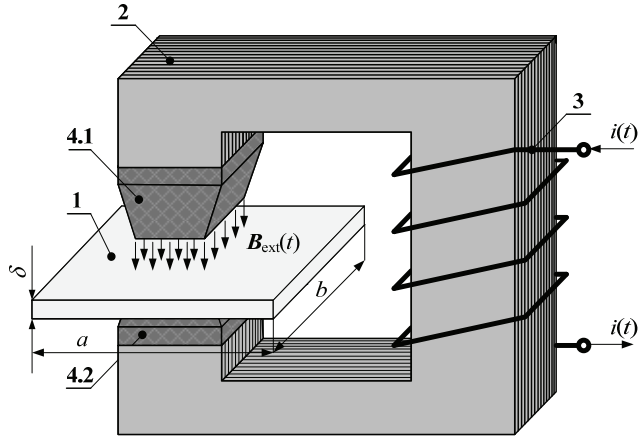

Fig. 1. Local induction heating of a very thin plate ($\delta << a,b$): **1**–locally heated thin nonferromagnetic plate, **2**–laminated magnetic circuit, **3**–field coil, **4.1** and **4.2**–ferromagnetic focusators

Handling such a problem as a geometrically 3D task (depending on quantities x, y, z, t), formulating it in the classical manner (in terms of magnetic vector potential $\boldsymbol{A}$) and solving it by the finite element method is practically unreal. This is because the thickness δ of the plate is negligible with respect to its remaining dimensions, which represents the fundamental complication for building the finite-element mesh.

On the other hand, considering the problem as a 2D task (thickness δ would be neglected) is also counterproductive because in this case it is not possible to numerically approximate the boundary conditions for the magnetic vector potential $\boldsymbol{A}$.

The paper solves the problem of induction heating of a circular nonmagnetic disk in a novel way. Distribution of eddy currents induced in the disk is described by means of electric vector potential $\boldsymbol{T}$ while the nonstationary temperature field is described in terms of heat sources and sinks. This eliminates the above difficulties and allows fast computing of results. The numerical solution is realized in a hard-coupled formulation.

Formulation of the problem

Consider a very thin, nonferromagnetic, electrically conductive circular disk of radius r_2, thickness $\delta \to 0$ (it must be substantially lower than the depth of penetration), electrical conductivity γ_{el}, and magnetic permeability μ_0, see Fig. 2. Its surface is denoted by symbol Ω and its boundary by symbol Γ.

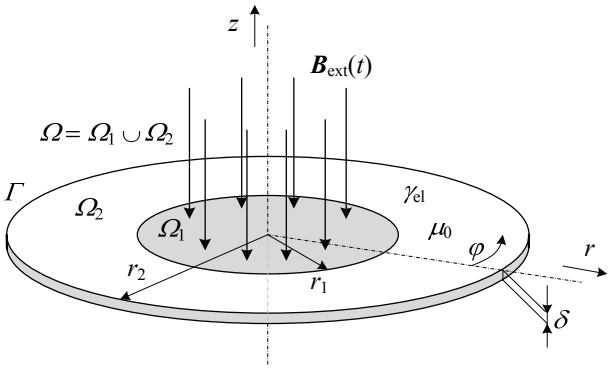

Fig. 2. Basic arrangement of the investigated circular disk

The disk is locally (in a circle $\Omega_1 \subset \Omega$ whose radius $r_1 < r_2$) exposed by a time variable external magnetic field $\boldsymbol{B}_{\mathrm{ext}}(r,t) = \mathbf{z}_0 B_{\mathrm{z,ext}}(r,t)$ and heated by the currents in-

duced in it (their density being denoted $\boldsymbol{J}_{\mathrm{ind}}$). The corresponding nonstationary temperature field affects the electrical conductivity γ_{el} (and also thermal conductivity and heat capacity of the disk), so that both mentioned fields are mutually coupled.

The task is to map the time evolution of distributions of induced currents, specific Joule losses and temperature along the radius of the disk.

Continuous mathematical model

The total magnetic flux density $\boldsymbol{B}$ in the system consists of two components: external flux density $\boldsymbol{B}_{\mathrm{ext}}$ and magnetic flux density $\boldsymbol{B}_{\mathrm{ind}}$ produced by currents of density $\boldsymbol{J}_{\mathrm{ind}}$ induced in the disk.

The total electric field strength $\boldsymbol{E}$ in the system follows from the second Maxwell equation

$$\operatorname{curl}\boldsymbol{E} = -\frac{\partial \boldsymbol{B}}{\partial t} = -\frac{\partial \boldsymbol{B}_{\mathrm{ext}}}{\partial t} - \frac{\partial \boldsymbol{B}_{\mathrm{ind}}}{\partial t} \tag{1}$$

As in the disk $\boldsymbol{J}_{\mathrm{ind}} = \gamma_{\mathrm{el}}\boldsymbol{E}$, we can write

$$\operatorname{curl}\frac{\boldsymbol{J}_{\mathrm{ind}}}{\gamma_{\mathrm{el}}} = -\frac{\partial \boldsymbol{B}}{\partial t}. \tag{2}$$

Both vectors $\boldsymbol{E}$ and $\boldsymbol{J}_{\mathrm{ind}}$ obviously have only one component in the circumferential direction, so that

$$\boldsymbol{E} = \boldsymbol{\varphi}_0 E_\varphi,\ \boldsymbol{J}_{\mathrm{ind}} = \boldsymbol{\varphi}_0 J_{\mathrm{ind},\varphi}. \tag{3}$$

Introduce now the electric vector potential $\boldsymbol{T}$ by relation

$$\boldsymbol{J}_{\mathrm{ind}} = -\operatorname{curl}\boldsymbol{T}. \tag{4}$$

It is clear (see (3)) that $\boldsymbol{T}(r,t) = \mathbf{z}_0 T_z(r,t)$. Hence,

$$\operatorname{curl}\left(\frac{1}{\gamma_{\mathrm{el}}}\operatorname{curl}\boldsymbol{T}\right) = -\operatorname{curl}\frac{\boldsymbol{J}_{\mathrm{ind}}}{\gamma_{\mathrm{el}}} = \frac{\partial \boldsymbol{B}}{\partial t} = \frac{\partial \boldsymbol{B}_{\mathrm{ext}}}{\partial t} + \frac{\partial \boldsymbol{B}_{\mathrm{ind}}}{\partial t}. \tag{5}$$

Neglecting the displacement currents in the first Maxwell equation (values of applied frequencies are supposed to be smaller than 10^6 Hz) we can write

$$\operatorname{curl}\boldsymbol{H}_{\mathrm{ind}} = \operatorname{curl}\frac{\boldsymbol{B}_{\mathrm{ind}}}{\mu_0} = \boldsymbol{J}_{\mathrm{ind}} \tag{6}$$

and using (4) we obtain

$$-\operatorname{curl}\boldsymbol{T} = \operatorname{curl}\frac{\boldsymbol{B}_{\mathrm{ind}}}{\mu_0}. \tag{7}$$

Hence, generally

$$-\boldsymbol{T} = \frac{\boldsymbol{B}_{\mathrm{ind}}}{\mu_0} - \operatorname{grad}\psi, \tag{8}$$

where ψ is any scalar function. But in our case, the quantity $\boldsymbol{T}$ represents the electric vector potential produced only by the induced magnetic flux density. That is why $\operatorname{grad}\psi = 0$.

On this assumption (5) may be rewritten as follows:

$$\operatorname{curl}\left(\frac{1}{\gamma_{\mathrm{el}}}\operatorname{curl}\boldsymbol{T}\right) = -\mu_0\frac{\partial \boldsymbol{T}}{\partial t} + \frac{\partial \boldsymbol{B}_{\mathrm{ext}}}{\partial t}. \tag{9}$$

Considering (3) and the aforementioned fact that $\boldsymbol{T}(r,t) = \mathbf{z}_0 T_z(r,t)$, we finally obtain

$$\frac{\partial}{\partial r}\left(\frac{1}{\gamma_{\mathrm{el}}}\right)\frac{\partial T_z}{\partial r} + \frac{1}{\gamma_{\mathrm{el}}}\frac{\partial^2 T_z}{\partial r^2} + \frac{1}{\gamma_{\mathrm{el}}}\frac{1}{r}\frac{\partial T_z}{\partial r} = \mu_0\frac{\partial T_z}{\partial t} - \frac{\partial B_{z,\mathrm{ext}}}{\partial t}, \tag{10}$$

which holds everywhere in region Ω. Of course, in region Ω_2 the external field $\boldsymbol{B}_{\mathrm{ext}}$ does not exist, so that the term $\partial B_{z,\mathrm{ext}}/\partial t$ vanishes there.

For the density of the induced currents $J_{\mathrm{ind},\varphi}$ we obtain from (4)

$$J_{\varphi,\mathrm{ind}} = -\frac{\partial T_z}{\partial r} \tag{11}$$

and the volumetric Joule losses are

$$w_{\mathrm{J}} = J_{\varphi,\mathrm{ind}}^2/\gamma_{\mathrm{el}}. \tag{12}$$

From the above formulas we can see two principal advantages of introducing the electric $\boldsymbol{T}$ potential for such kinds of problems:

- Potential $\boldsymbol{T}$ is defined only in electrically conductive domains, in our case only in the disk. On the other hand, magnetic vector potential $\boldsymbol{A}$ would have to be determined everywhere in the whole system (i.e., inductor, magnetic cores, focusators, ambient air), which would require much larger 3D mesh. Transversal discretization of the thin disk would be, moreover, very complicated. The only drawback is that the currents induced in the disk have the same density along its thickness
- The boundary conditions for the electric vector potential $\boldsymbol{T}$ are very simple, because the normal component of the induced current densities $\boldsymbol{J}_{\mathrm{ind}}$ along the boundary Γ of the disk vanishes. This means

$$\frac{\partial \boldsymbol{T}}{\partial \tau} = \mathbf{0},$$

where τ is the tangential direction to boundary Γ at its arbitrary point. In other words, the value of $\boldsymbol{T}$ along the boundary Γ is a constant, and as before the heating process there is no magnetic field in the system, we can put $\boldsymbol{T}(\Gamma) = \mathbf{0}$. On the other hand, finding the value of the magnetic vector potential $\boldsymbol{A}$ along the boundary Γ is impossible and for solution we would have to introduce a sufficiently distant artificial boundary with the Dirichlet condition.

- Potential $\boldsymbol{T}$ is advantageous for the solution of coupled electromagnetic-thermal problems similarly as the magnetic vector potential $\boldsymbol{A}$. From its distribution one can easily derive the density of induced currents $\boldsymbol{J}_{\mathrm{ind}}$ and volumetric Joule losses w_{J} necessary for the consequent thermal computations.

For computation of the nonstationary temperature field it is advantageous to describe the thermal balance of the disk in terms of heat sources (volumetric Joule losses) and sinks (convection and radiation from both its sides), see Fig. 3.

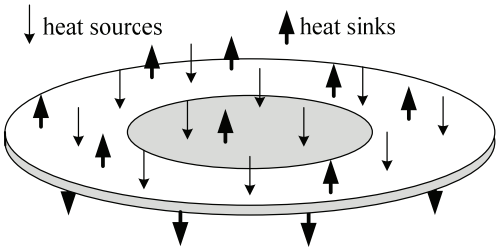

Fig. 3. Heat sources and sinks in the disk

Using this approach the heat-transfer equation may be written in the form

$$\frac{\partial\lambda}{\partial r}\frac{\partial T}{\partial r}+\lambda\frac{\partial^2 T}{\partial r^2}+\lambda\frac{1}{r}\frac{\partial T}{\partial r}=\rho c\frac{\partial T}{\partial t}-w_{\mathrm{J}}+ \\ +\frac{1}{\delta}\left[\left(\alpha_{\mathrm{c},1}+\alpha_{\mathrm{c},2}\right)\left(T-T_{\mathrm{ext,c}}\right)+2\varepsilon_{\mathrm{SB}}C_{\mathrm{r}}\left(T^4-T_{\mathrm{ext,r}}^4\right)\right], \tag{13}$$

where λ, ρ, c are the temperature-dependent thermal conductivity, specific mass and specific heat, respectively, $\varepsilon_{\mathrm{SB}}$ is the Stefan-Boltzmann constant, C_{r} is the coefficient of emissivity, $T_{\mathrm{ext,c}}$, $T_{\mathrm{ext,r}}$ are the distant temperatures for simulation of convection and radiation and, finally, $\alpha_{\mathrm{c},1}$ and $\alpha_{\mathrm{c},2}$ are the coefficients of convective heat transfer along the upper and lower sides of the disk. Now the boundary condition is given by zero thermal flux (the thickness δ of the disk is considered negligible) from the boundary Γ of the disk.

Numerical solution

The system consisting of coupled nonlinear parabolic-type partial differential equations (10) and (13) (defined on 1D domain $0\le r\le r_2$) was solved numerically by the finite difference method using explicit approximation of accuracy $O\left[\left(\Delta r\right)^2+\Delta t\right]$ [7]. We checked both convergence and numerical stability of the solution. The stability is determined by the von Neumann condition [8] in the form $\Delta t\le\left(\Delta r\right)^2/\sigma$, where in (10) $\sigma=1/\gamma_{\mathrm{el}}\mu_0$, while in (13) $\sigma=\lambda/\rho c$. The code developed by the authors was written in Free Pascal [9].

Illustrative example

An aluminum circular disk of $r_2=0.1$ m is exposed (in a region $\Omega_1\approx 0\le r\le r_1$, where r_1 may vary in some limited range, similarly as the thickness δ) by harmonic magnetic field $B_{z,\mathrm{ext}}\left(t\right)=B_0\sin\left(2\pi ft\right)$, where B_0 and frequency f also can vary.

The physical properties of pure aluminum are nonlinear functions of the temperature. For example, Fig. 4 depicts the dependence $\lambda=\lambda\left(T\right)$, taken over from [10].

At first we carefully tested the convergence and stability of the results. Fig. 5 shows the convergence curves for electric vector potential T_z and volumetric Joule losses w_{J} at a given radius. It is clear that for the number of nodes $n>100$ the changes decrease fast. The convergence of the temperature for the specified geometry and other input data is shown in Fig. 6. Even in this case, the results well converge for $n>100$.

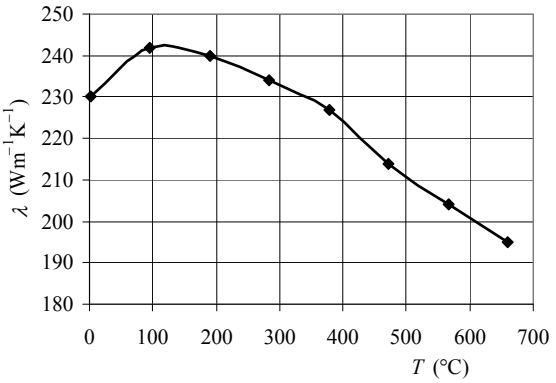

Fig. 4. Dependence $\lambda=\lambda\left(T\right)$ for pure aluminum

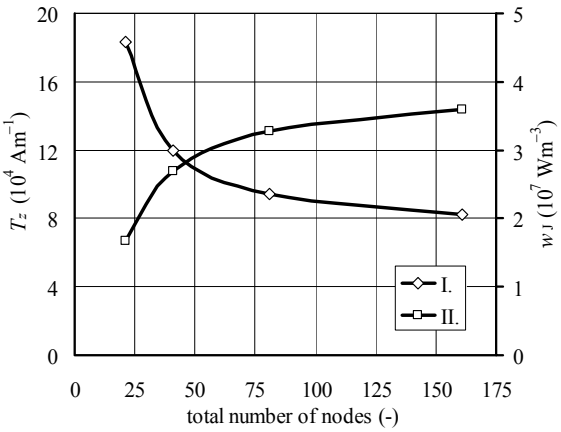

Fig. 5. Convergence curves for electric vector potential $T_z\left(r,t\right)$ (I.) and volumetric Joule losses $w_{\mathrm{J}}\left(r,t\right)$ (II.) for $r=0.02$ m after 10 periods ($r_1=0.02$ m, $\delta=0.001$ m, $B_0=1$ T, $f=50$ Hz)

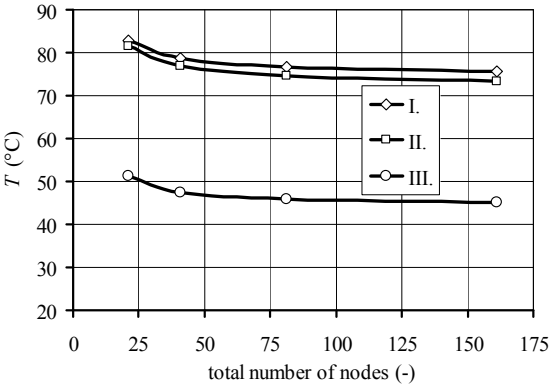

Fig. 6. Convergence curves for the temperature T at three different radii after 60 s of heating for $r_1=0.02$ m, $\delta=0.001$ m, $B_0=1$ T, $f=50$ Hz (I. r = 0 m, II. r = 0.02 m, III. r = 0.1 m)

Figure 7 shows the distribution of the component T_z of the electric vector potential along the radius of the disk of specified parameters excited by harmonic external magnetic field ($B_0=1$ T, $f=50$ Hz) after $t=0.42$ s obtained for different time steps (I – instable for time step $\Delta t=0.0006$ s, II – stable for time step $\Delta t=0.0004$ s, the limit of stability being about $\Delta t=0.0004713$ s).

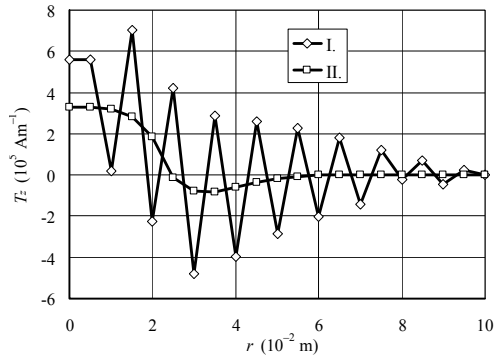

Fig. 7. Distribution of electric vector potential T_z along the radius of the disk ($r_1 = 0.02$ m, $\delta = 0.001$ m, $t = 0.42$ s): I – instable solution, II – stable solution

Then we started investigating various characteristics of the system. For example, Fig. 8 shows the distribution of temperature along the radius of the disk for different times. It is clear that the domain of the highest temperature can be found between the focusators (a thin air gap with rather high temperature of air, very low convection).

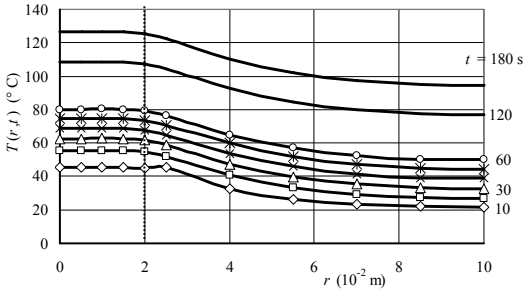

Fig. 8. Distribution of the temperature in the thin aluminum circular disk ($r_1 = 0.02$ m, $\delta = 0.001$ m, $B_0 = 1$ T, $f = 50$ Hz)

Figure 9 depicts such the time evolution of temperature for varying radius r_1 of the part exposed to the external magnetic field.

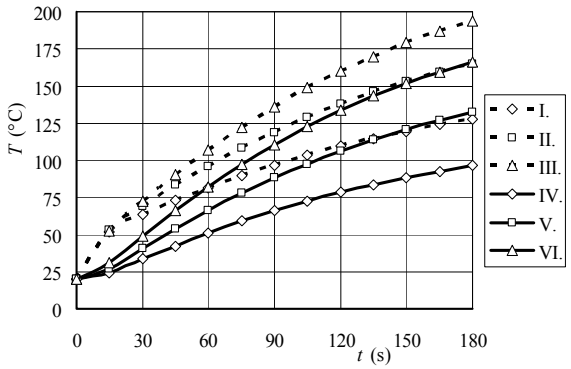

Fig. 9. Time evolution of the temperature at two radii for varying radius r_1 (r_2 = 0.1 m, $\delta = 0.001$ m, $B_0 = 1$ T, $f = 50$ Hz):
I. $r = r_1$, $r_1 = 0.02$ m, II. $r = r_1$, $r_1 = 0.03$ m, III. $r = r_1$, $r_1 = 0.04$ m, IV. $r = r_2$, $r_1 = 0.02$ m, V. $r = r_2$, $r_1 = 0.03$ m, VI. $r = r_2$, $r_1 = 0.04$ m

Finally, Fig. 10 shows a set of analogous graphs for varying frequency f of the external field. The dependence is for higher temperatures approximately linear (which means that an increase of frequency leads to a proportional temperature rise).

Numerous similar graphs were obtained for other changing parameters.

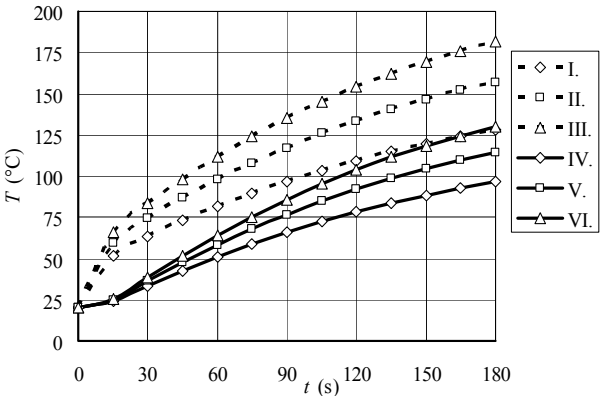

Fig. 10. Time evolution of the temperature at two radii for varying frequency f : ($r_1 = 0.02$ m, r_2 = 0.1 m, $\delta = 0.001$ m, $B_0 = 1$ T)
I. $r = r_1$, $f = 50$ Hz, II. $r = r_1$, $f = 75$ Hz, III. $r = r_1$, $f = 100$ Hz,
IV. $r = r_2$, $f = 50$ Hz, V. $r = r_2$, $f = 75$ Hz, VI. $r = r_2$, $f = 100$ Hz

Conclusion

Electric vector potential seems to be a powerful tool for modeling induction heating in systems characterized by geometrically incommensurable elements, because it allows handling specific 3D arrangements as 2D problems. Another advantage consists in the formal similarity of equations for the electric vector potential and magnetic vector potential, which makes possible to use classical FEM codes for numerical computation of such tasks.

Next work in the field will be aimed at the process of thermoelastic displacements in the heated disk.

Acknowledgement

The financial support of the Grant Agency of the Czech Republic (project No. 102/09/1305) and Research Plan MSM 6840770017 is gratefully acknowledged.

REFERENCES

[1] Rudnev V. I., Loveless D., Cook R., Black M., *Handbook of Induction Heating*, CRC Press, New York, 2002.
[2] Zinn S., Semiatin S. L., *Elements of Induction Heating: Design, Control, and Applications,* ASM International, USA, 1988.
[3] Rapoport E., Pleshivtseva Y., *Optimal Control of Induction Heating Processes*, CRC Press, Boca Raton, FL, USA, 2007.
[4] www.vectorfields.com.
[5] www.ansys.com.
[6] www.cedrat.com.
[7] Morton K.W., Mayers D.F., *Numerical Solution of Partial Differential Equations*, 2nd edition, Cambridge, UK, 1995.
[8] Samarskij A. A., Gulin A. V., *Ustojčivosť Raznostnych Schem*. Nauka, Moskva, 1973 (in Russian).
[9] www.freepascal.org.
[10] Database of material parameters http://www.jahm.com.

***Authors**: Prof. Ing. Ivo Doležel, CSc., Academy of Sciences of the Czech Republic, Institute of Thermomechanics, v.v.i., Dolejškova 5, 182 00 Praha 8, Czech Republic, E-mail: dolezel@it.cas.cz, Assoc. Prof. Bohuš Ulrych, CSc, University of West Bohemia, Faculty of Electrical Engineering, Univerzitní 23, 306 14 Plzeň, Czech Republic, E-mail: ulrych@kte.zcu.cz, Ing. Petr Kropík, Ph.D., University of West Bohemia, Faculty of Electrical Engineering, Univerzitní 23, 306 14 Plzeň, Czech Republic, E-mail: pkropik@kte.zcu.cz,*